Title

Analysis of linearity of highly saturated electroabsorption modulator link due to photocurrent feedback effect

Journal

Optics Express, 15(14)

ISSN

1094-4087

Authors

Chang, W. S. C.
Shubin, I.
Yu, P. K. L.
et al.

Publication Date

2007-07-01

Peer reviewed

Analysis of linearity of highly saturated electroabsorption modulator link due to photocurrent feedback effect

X. B. Xie, I. Shubin, W. S. C. Chang, and P. K. L. Yu

University of California at San Diego, La Jolla, CA 92093
yu@ece.ucsd.edu

Abstract: We have analyzed the linearity performance of analog fiber-optic links based on electroabsorption modulators (EAM) operating at high optical power. The negative feedback caused by photocurrent generation improves the modulator linearity in the gain saturation regime. In the absence of laser relative intensity noise (RIN), the link spur-free dynamic range (SFDR) increases with the power of four-thirds of the input optical power after gain saturation occurs. A multi-octave SFDR of more than 135 $dB/Hz^{2/3}$ has been found to be achievable with sufficiently high power.

Keywords: (060.2360) Fiber optics links and subsystems; (130.5990) Semiconductors; (250.7360) Waveguide modulators; (350.4010) Microwaves; (999.9999) Spur-free dynamic range; (999.9999) Negative feedback.

References and Links

1. W. B. Bridges, U. V. Cummings, and J. H. Schaffner, "Linearized modulators for analog photonic links," in *MWP '96 Technical Digest, International Topical Meeting on Microwave Photonics*, (Institute of Electrical and Electronics Engineers, , New York, 1996), pp. 61–64.
2. G. E. Betts, X. B. Xie, I. Shubin, W. S. C. Chang, and P. K. L. Yu, "Gain limit in analog links using electroabsorption modulators," IEEE Photon. Technol. Lett. **18**, 2065–2067 (2006).
3. C. H. Cox III, E. I. Ackerman, G. E. Betts, and J. L. Prince, "Limits on the performance of RF-over-fiber links and their impact on device design," IEEE Trans. Microwave Theory Tech. **52**, 906–920 (2006).
4. T. H. Lee, *The Design of CMOS Radio-Frequency Integrated Circuits* (Cambridge Univ. Press, 1998), Chap. 14.
5. R. B. Welstand, S. A. Pappert, C. K. Sun, J. T. Zhu, Y. Z. Liu, and P. K. L. Yu, "Dual-function electroabsorption waveguide modulator/detector for optoelectronic transceiver applications," IEEE Photon. Technol. Lett. **8**, 1540–1542 (1996).
6. K. J. Williams, L. T. Nichols, and R. D. Esman, "Photodetector nonlinearity limitations on a high-dynamic range 3 GHz fiber optic link," IEEE J. Lightwave Technol. **16**, 192–199 (1998).
7. E. I. Ackerman, "Broad-band linearization of a Mach-Zehnder electrooptic modulator," IEEE Trans. Microwave Theory Tech. **47**, 2271–2279 (1999).
8. P. K. L. Yu, I. Shubin, X. B. Xie, Y. Zhuang, A. J. X. Chen, and W. S. C. Chang, "Transparent ROF link using EA modulators," in *MWP '05 Technical Digest, International Topical Meeting on Microwave Photonics*, (Institute of Electrical and Electronics Engineers, Seoul, 2005), pp. 21–24.

1. Introduction

In commercial and military applications, analog fiber-optic links have been used to transmit radar as well as cable television (CATV) signals. The linearity of links is critical in the overall performance of the signal transmission. Among the components of a fiber-optic link, the linearity of optical modulator is of primary importance and has been broadly studied for improving the link linearity. Commonly the dc optical transfer curve of the modulator is used to estimate the linearity degradation during modulation. A small single sinusoidal signal applied at a bias point generates not only the fundamental signal but also its harmonics due to the non-linearity of optical transfer curve. Electro-optic modulator (EOM), such as widely used Mach-Zehnder modulator (MZM), usually has a well characterized and stable optical

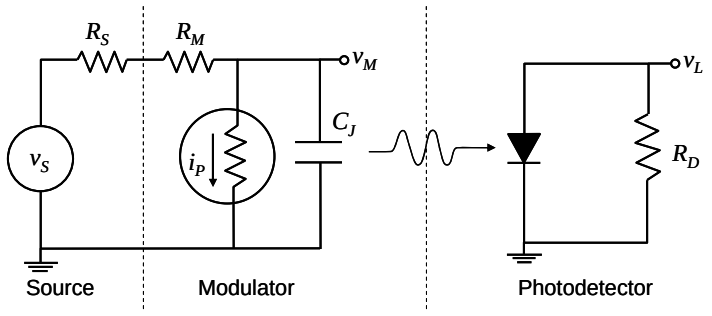

Fig. 1. An equivalent circuit model of EAM used in an analog fiber-optic link.

transfer curve. This eases the modeling and demonstration of combination of multiple MZMs for canceling high order harmonics and thus improving the link linearity [1]. In contrast, the optical transfer curve of an electroabsorption modulator (EAM) is dependent on both material properties and the device structure and cannot be easily described analytically. Therefore, it becomes very complicated to employ similar schemes to linearize an EAM link.

The intermodulation distortions of an analog fiber-optic link can be measured using the two-tone test. Two radio frequency (RF) tones f_1 and f_2 with a small frequency offset modulate the optical carrier. The second- and third- order intermodulation (IM2 and IM3) distortion signals are measured at the link output. The widely used figure of merit, spur-free dynamic range (SFDR), is defined as the output signal to noise ratio (SNR) as the IM3 signal starts to emerge from the noise floor. SFDR not only depends on the linearity of the optical transfer curve, but also on the link gain and link noise performance.

The link gain saturation and noise performance of EAM at high input optical power has been theorized and characterized by Betts *et al* [2]. The conclusion was that the voltage reduction across the modulation layer, as a result of the negative feedback effect generated by the photocurrent, causes the link gain to deviate from the quadratic dependence on input optical power and to finally approach a gain limit. Apparently the same mechanism also affects the EAM linearity. Regarding the link gain, experiments have shown the dominance of circuit photocurrent on the feedback effect [2]. Other effects such as carrier transport and thermal effects play only very minor roles. The factors that influence EAM link linearity, however, are more complicated. The photocurrent feedback effect can be a main contribution factor for certain designs, and an experimental study will be needed to understand it fully. In this letter, we analyze the linearity performance solely due to the photocurrent feedback effect and then discuss the possible implications when other factors are added. The result shows an input third-order intercept point (IIP3) dependence on third-order power of optical power at substantially high power, which overrides linearly dependent noise increase. The SFDR of the link is thus expected to improve with increased optical power. We also compare the SFDR performance of EOM and EAM links at high optical power.

2. Analysis

The small signal circuit model of the EAM can be represented similarly as in [1] which is shown here in Fig. 1, along with the optical signal transmission from the optical modulator to the photodetector. To simplify the equation derivation without loss of generality, the modulator termination resistance is not included here. The junction capacitance C_J is omitted in the following analysis for low frequency operation. As the input optical power is increased, both dc and ac photocurrent generation increase. This increases the portion of the voltage drop on the source resistance R_S and the EAM serial resistance R_M relative to the total source voltage, leaving a smaller portion on the modulator layer. From a feedback point of view, what happens at the EAM parallels a negative feedback system. The incoming voltage v_S

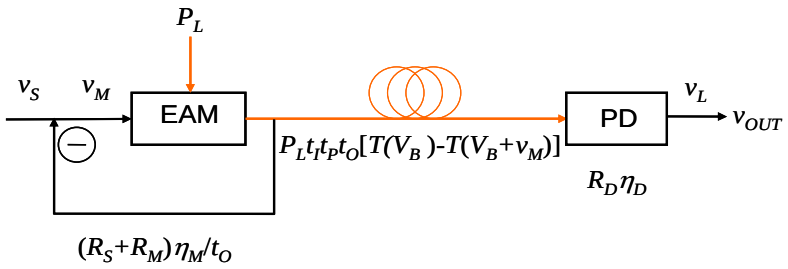

Fig. 2. Negative feedback system formed by the effect of photo-generated current on EAM circuit in an analog fiber-optic link configuration. The black and orange lines correspond to electrical and optical transmissions, respectively.

modulates the active layer and leads to the intensity modulation of the optical carrier, expressed as $P_L t_I t_P t_O[T(V_B)-T(V_B+v_M)]$, where $T(V)$ is the optical transfer function of the EAM; P_L, t_I, t_P, t_O, V_B and v_M are the input laser power, EAM input coupling coefficient, EAM propagation loss, EAM output coupling coefficient, the dc bias voltage, and the effective ac voltage across the modulation layer, respectively. At the same time the modulated light generates ac photocurrent which effectively reduces the voltage across the junction. At steady state, it becomes a negative feedback system, the output of which is coupled into the photodetector and generates output voltage v_L across load resistance R_D. This description can be schematically shown in Fig. 2, where η_M and η_D denote the responsivity of EAM and photodetector, respectively. With a low input optical power to the EAM, the photocurrent feedback can be ignored and the linearity of the electro-to-optical conversion is mainly determined by that of the optical transfer function $T(V)$. When the optical power increases, the effective voltage across the EAM junction is no longer v_S, but v_M which is modified by the photocurrent feedback. We can easily show that v_M satisfies the following equation:

$$v_M = v_S - (R_S + R_M)\eta_M P_L t_I t_P [T(V_B) - T(V_B + v_M)] \tag{1}$$

Using a voltage gain function $v_{OUT} = g(v_{IN})$ at no feedback, we can relate v_{IN} and v_{OUT} under feedback as follows:

$$g(v_{IN} - f v_{OUT}) = v_{OUT} \tag{2}$$

where g is a function that includes the nonlinear harmonics caused by the optical transfer curve $T(V)$ and f is the negative feedback coefficient as described by:

$$f = \frac{(R_S + R_M)\eta_M}{2\eta_D R_D t_O} \tag{3}$$

Here $v_{IN} = v_S/2$ is used to conform with the conventional definition for analog fiber-optic link gain, where the input RF power is taken with a modulator load matched to that of the RF source [3]. The output voltage v_{OUT} is equivalent to v_L, the ac voltage across the load resistance of the photodetector. It has been well established in electronic amplifier design that the negative feedback can improve the linearity of the whole system if the feedback coefficient is more linear than the transfer function of the system under no feedback [4]. When the loop voltage gain is large, the overall feedback system response is close to the inverted feedback network response. In our case, g represents the transfer function at no feedback and includes optical transfer curve nonlinearities. Feedback coefficient f, on the other hand, does not consist of any elements of the nonlinear optical transfer curve. When the voltage gain at no feedback ($f = 0$) is high enough, the actual voltage gain (under feedback)

can be approximated as 1/*f*. The system linearity is hence determined mainly by *f*, and not by the EAM transfer function. However, the EAM and photodetector responsivities involved in *f* can still affect the system linearity.

The implications of the photocurrent feedback on this fiber-optic link linearity can also be analyzed by separating the intrinsic and extrinsic optical transfer curves. We define intrinsic optical transfer curve as a function of junction voltage $T(V_M)$. It depends on material properties and does not include any circuit effects. It is clear that the aforementioned optical transfer curve is equivalent to our intrinsic optical transfer curve definition. The extrinsic optical transfer curve $Te(V_{IN})$ is dependent on $v_{IN} = v_S/2$, $Te(V_{IN})$ includes negative photocurrent feedback effect and governs the linearity when EAM gain is saturated. Different orders of derivatives of both intrinsic and extrinsic optical transfer curves with respect to their arguments can be evaluated and related based upon the above equivalent circuit model:

$$\frac{dT_e}{dV_{IN}} = \frac{2\dfrac{dT}{dV_M}}{1 - P_L t_I t_P \eta_M \left(R_S + R_M\right)\dfrac{dT}{dV_M}} \tag{4}$$

$$\frac{d^2T_e}{dV_{IN}^{\ 2}} = \frac{4\dfrac{d^2T}{dV_M^{\ 2}}}{\left(1 - P_L t_I t_P \eta_M \left(R_S + R_M\right)\dfrac{dT}{dV_M}\right)^3} \tag{5}$$

$$\frac{d^3T_e}{dV_{IN}^{\ 3}} = \frac{8\dfrac{d^3T}{dV_M^{\ 3}}\left(1 - P_L t_I t_P \eta_M \left(R_S + R_M\right)\dfrac{dT}{dV_M}\right) + 24 P_L t_I t_P \eta_M \left(R_S + R_M\right)\left(\dfrac{d^2T}{dV_M^{\ 2}}\right)^2}{\left(1 - P_L t_I t_P \eta_M \left(R_S + R_M\right)\dfrac{dT}{dV_M}\right)^5} \tag{6}$$

Eq. (4) is the relationship between first order derivatives of the transfer curves. It accounts for the link gain saturation as detailed in [2]. The term dT/dV_M is considered negative due to the fact that larger voltage causes less optical transmission in conventional quantum well designs. The denominator on the right side of Eq. (4), denoted as EAM saturation factor *k*, becomes much larger than unity when the input optical power is high enough, which reduces the link gain:

$$k = 1 - P_L t_I t_P \eta_M \left(R_S + R_M\right)\frac{dT}{dV_M} = 1 + \frac{P_L t_I t_P \eta_M \left(R_S + R_M\right)\pi}{2V_\pi} \tag{7}$$

where V_π is the EAM equivalent half wave voltage defined as $(\pi/2)(dT/dV_M)^{-1}$. Eqs. (5) and (6) represent higher order derivatives of optical transfer curves. The derivatives of extrinsic and intrinsic optical transfer curves are related by a factor of k^3 for the second order, and k^4 for the third order when EAM is biased at its largest slope efficiency voltage point where the second order derivative nulls out. The second order null point is also the bias point for multi-octave operation. It is clear that the derivatives of extrinsic optical transfer curves become much smaller than that of intrinsic optical transfer curves when the saturation factor $k >> 1$.

The link linearity due to the modulator transfer curve can be analyzed by expanding it to different orders, yielding the input second- and third-order intercept points (IIP2 and IIP3) as:

$$\mathrm{IIP2} \propto \left(\frac{dT}{dV} \Big/ \frac{d^2T}{dV^2}\right)^2 \quad \text{and} \quad \mathrm{IIP3} \propto \frac{dT}{dV} \Big/ \frac{d^3T}{dV^3} \tag{8}$$

Consequently, IIP2 and IIP3 of highly saturated EAM link can be improved by a factor of k^4 and k^3 compared with the no-feedback situation. The output second and third-order intercept points (OIP2 and OIP3) increases by the same factor when the gain saturates. On the other hand, the link output noise only increases linearly with optical power even when EAM shot noise dominates in the saturation case, which is approximately proportional to k. Hence, in the absence of laser intensity noise (RIN), the link SFDR improves by $k^{4/3}$.

The discussion carried out so far compares linearity performance of the EAM link with and without photocurrent feedback effect, both under high optical power when link gain saturates. Although the observed high power operation of EAM has already the photocurrent feedback built-in, a view from the no-feedback perspective gives us more insight in understanding the involved mechanism. The evaluation of the EAM link linearity change from low optical power state to high optical power state would require knowledge not only of the difference between intrinsic and extrinsic optical transfer curves at high optical power but also of the intrinsic optical transfer curve change as the optical power increases, which involves a variety of effects that can modify material absorption properties. If we assume the change of the intrinsic transfer curve imposes only minor effect on the link linearity compared with the feedback effect and also exclude the nonlinearities of the EAM and photodetector responsivities, we can calculate the link performance based on the IIP3 value of the EAM at low power. Fig. 3 shows the dependence of the link multi-octave IIP3 and output noise floor on input optical power in the absence of the laser RIN. A low power IIP3 of 20 dBm is assumed [5]. The calculation clearly shows faster increase of IIP3 than link output noise at high optical power levels. Fig. 4 shows the dependence of RF link gain, multi-octave OIP3 and SFDR on input optical power. Before the EAM experiences gain saturation, the OIP3 increase is mainly due to the gain increase. At high power, the EAM link gain does not increase substantially but IIP3 starts to rise up rapidly. The OIP3 thus keeps increasing. As mentioned before, the link output noise does not increase faster than OIP3, therefore the link SFDR keeps improving as the input optical power is raised. At optical power of more than 700 mW, SFDR can reach 135 dB/Hz$^{2/3}$.

The derivation of Eqs. (4)-(6) assumes η_M and η_D to be constants with respect to the input voltage, which is the ideal case. In practice, a complete calculation should include

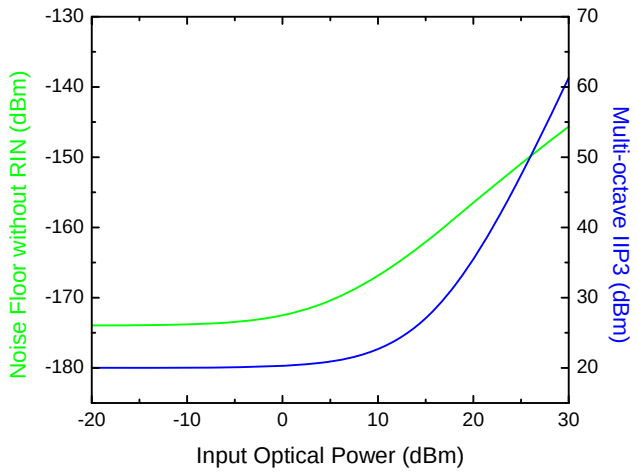

Fig. 3. Calculated link output noise floor and multi-octave IIP3 as a function of input optical power. Laser RIN noise is not included. Low power EAM IIP3 of 20 dBm is assumed. Additional optical loss of 3 dB is caused by dc bias . Other parameters used in the calculation are: $t_I = t_O$ = -3 dB, t_P = -1 dB, $R_S = R_D$ = 50 Ω, R_M = 5 Ω, $\eta_M = \eta_D$ = 1 A/W, V_π = 1.5 V.

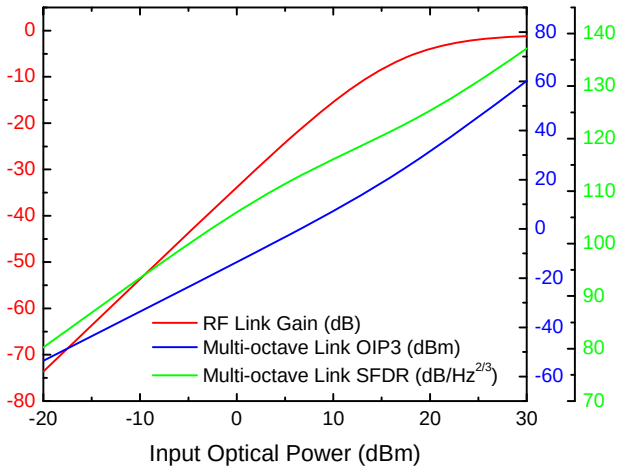

Fig. 4. Calculated RF link gain, multi-octave link OIP3 and SFDR dependence on input optical power. Conditions and parameter values in the calculation are the same as Fig. 3.

nonlinearities of η_M and η_D as well. More studies are needed for a better understanding of the dependences of η_M and η_D upon input voltage at high optical power before their effects on link linearity can be evaluated.

Compared with EOM links, SFDR improvement of EAM links at increased input optical power is due to a different mechanism. In EOM links, IIP3 stays constant as optical power is raised. The SFDR improvement comes from faster increase of link gain over link noise floor. In the absence of RIN, SFDR of EOM links improves only by a power of two-thirds of the increased optical power. This is much less than a power of four-thirds as for the case of EAM links at high power. With RIN involved, SFDR of EOM links will finally reach a limit as optical power is raised. In contrast, SFDR of EAM links will keep increasing.

SFDR of single MZM link is mainly limited by its nonlinear transfer curve. Experimental result showed a multi-octave SFDR of only 119.5 dB/Hz$^{2/3}$ at 240 mW laser power [6]. Linearized EOM links can improve sub-octave SFDR to be beyond 130 dB/Hz$^{4/5}$. However, the multi-octave SFDR remained low. A dual-wavelength EOM scheme with optical powers of 200 mW at 1320 nm and 30 mW at 1550 mW yielded an SFDR of 121 dB/Hz$^{2/3}$ [7]. These numbers are lower than what we estimated for a high power EAM link.

As high power components such as low RIN doped-fiber laser, optical amplifier, EAM, and photodetector are readily available [3,8], the realization of the high SFDR EAM link analyzed above can still be challenging due to added noise from optical amplifier and fiber nonlinearities such as stimulated Brillouin scattering (SBS) and four-wave mixing (FWM).

3. Conclusions

We have analyzed linearity of EAM fiber link at high optical power as the link gain saturates. This involves a negative feedback system which turns out to improve link linearity even when the link gain saturates. By comparing the EAM intrinsic and extrinsic optical transfer curves, the link multi-octave OIP3 and SFDR are derived to increase with k^3 and $k^{4/3}$, respectively.

Acknowledgments

The authors acknowledge the funding support of Defense Advanced Research Projects Agency via Photonic Systems Inc., AFRL at Rome location, and Lockheed Martin at Newtown, Penn.